**Supplementary Figures**

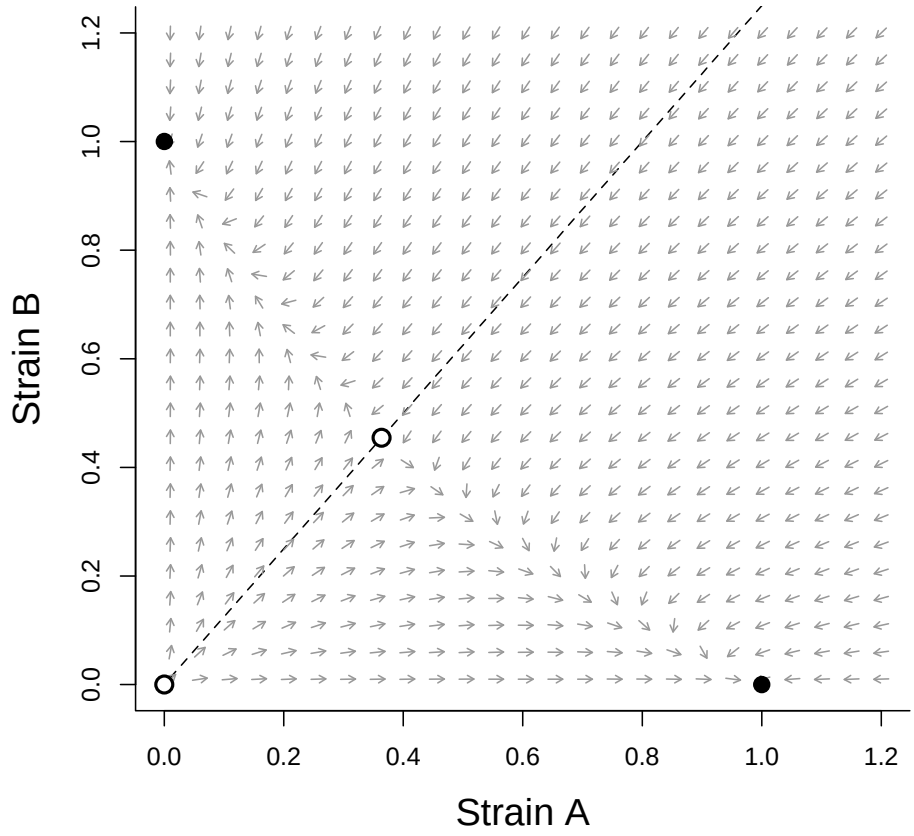


**Supplementary Figure 1. Illustration of T6SS mediated dynamics in a well-mixed population.** Arrows indicate the direction of the dynamics for any given combination of densities of strains *A* and *B*. Open circles indicate the unstable equilibria, while closed circles are stable equilibria. The dashed line indicates the critical ratio of strains *A* and *B* dictating which stable equilibrium will be reached. Parameter values are $r = 2$, $s = 2$, $\alpha_{AB} = 0.8$ and $\alpha_{BA} = 1$. Note that for these parameter the basin of attraction for the equilibrium where *A* dominates ($A = r/s$, $B = 0$) is larger than the basin of attraction for the equilibrium where *B* dominates ($A = 0$, $B = r/s$) owing to *A*'s superior killing ability ($\alpha_{BA} > \alpha_{AB}$).

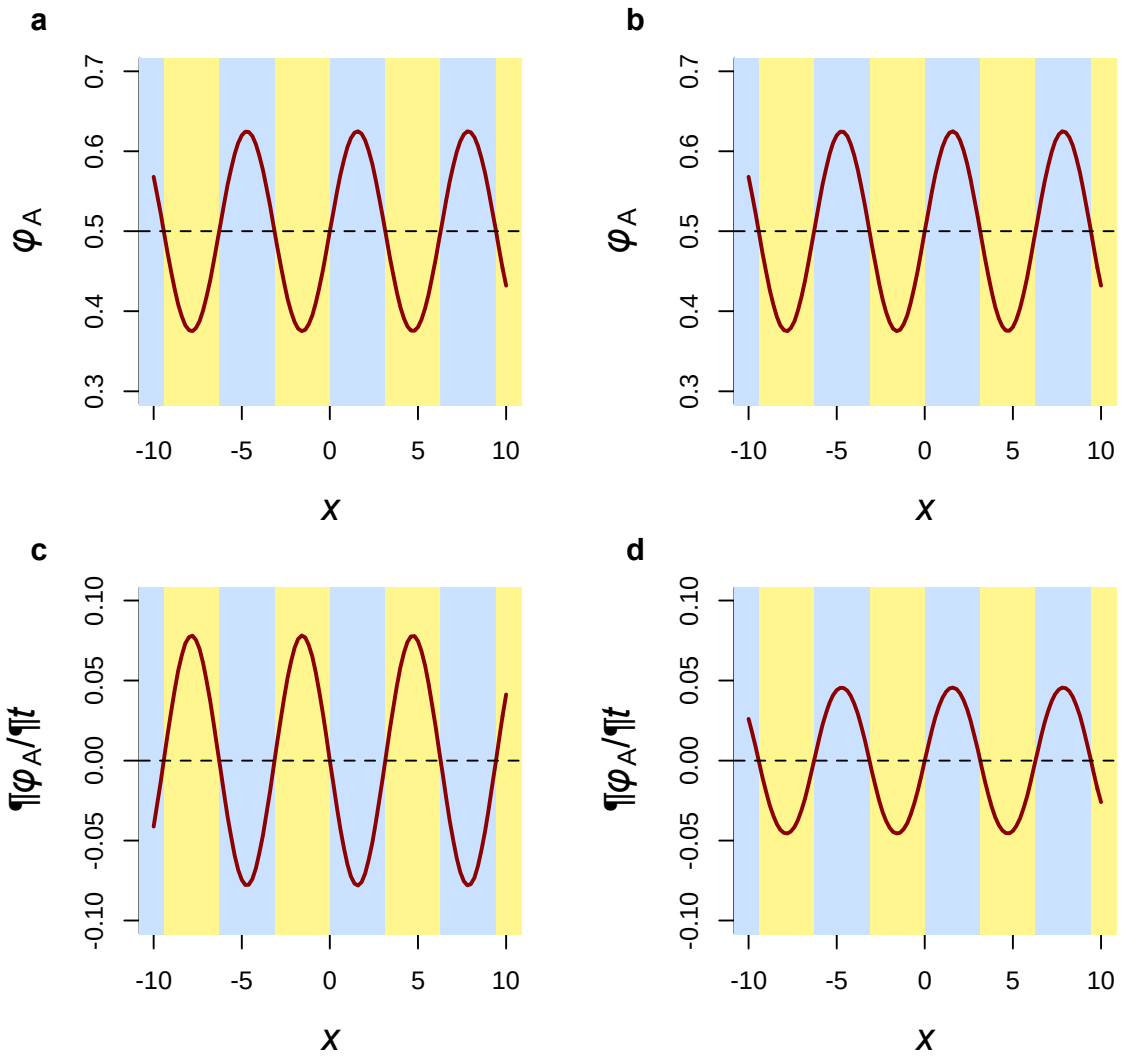


**Supplementary Figure 2. Illustration of spatial decomposition of mixed equilibrium in one dimension.** Plotted are the proportion of cells of strain *A* ($\varphi_A$) in (a) and (b), and the rate of change in this proportion ($\partial\varphi_A/\partial t$) in (c) and (d) along a spatial axis *x*. The different shaded regions indicate regions of positive (blue) and negative (yellow) fluctuation in composition. In (a) and (c) a high rate of bacterial dispersal/diffusion ($d$ = 1) through space means that the fluctuation in the density of *A* is on narrow a scale relative to bacterial dispersal/diffusion and the system will return towards the spatially homogenous equilibrium ($\partial\varphi_A/\partial t$ and $\varphi_A$ are of opposite sign) as bacterial/dispersal diffusion is strongly homogenising. However, in (b) and (d) when the bacterial dispersal/diffusion rate is lower ($d$ = 0.01) the spatial fluctuations occur on a wider scale relative to bacterial dispersal/diffusion and the system will be begin to decompose into areas divergent in composition ($\partial\varphi_A/\partial t$ and $\varphi_A$ are of opposite sign) as bacterial dispersal/diffusion is a relatively weak force compared to the demographic effects of killing. Other parameter values are $r$ = 2, $s$ = 2, $\alpha_{AB}$ = 1, $\alpha_{BA}$ = 1, $a$ = 0.1 and $\beta$ = 1.

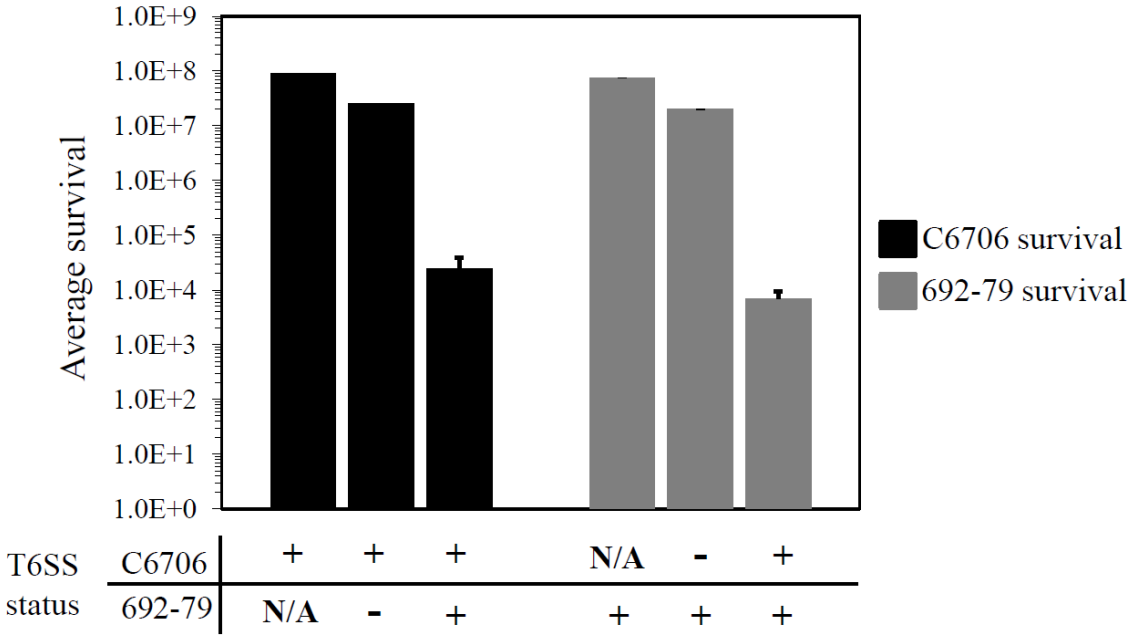


**Supplementary Figure 3. *Vibrio cholerae* strains C6706 and 692-79 are mutual killers**. Spectinomycin resistant C6706 survival was measured after a 3 hour incubation on membrane filters on LB agar in a 1:10 ratio with LB broth[1], or liquid cultures of 692-79 T6SS$^-$ (Δ*vasK*), or 692-79 T6SS$^+$ strains and is represented by black bars. Kanamycin resistant 692-79 survival was measured similarly in a 1:10 ratio with LB broth, C6706 T6SS$^-$ (Δ*vask*), or C6706 T6SS$^+$ and is represented by gray bars. Shown are average prey survival values ± one standard deviation after triplicate encounters. One representative experiment is shown of three performed.

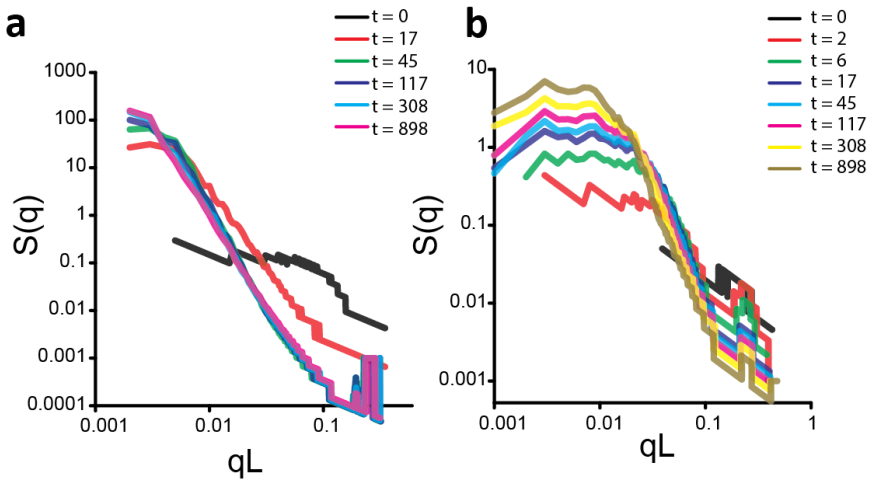


**Supplementary Figure 4. Structural analysis of additional models**. The static structure factor, *S(q)*, is plotted at different times versus wavenumber, *q*, multiplied by cell size, *L*, for the PDE model with diffusion $d = 0.01$ (a) and the Ising model with Glauber spin flip dynamics on the square lattice (b). In both the PDE and Ising spin models, *S(q)* increases at small *q* as time increases, just as was seen for the individual based model and experiments in Figure 2a and b, respectively**.**

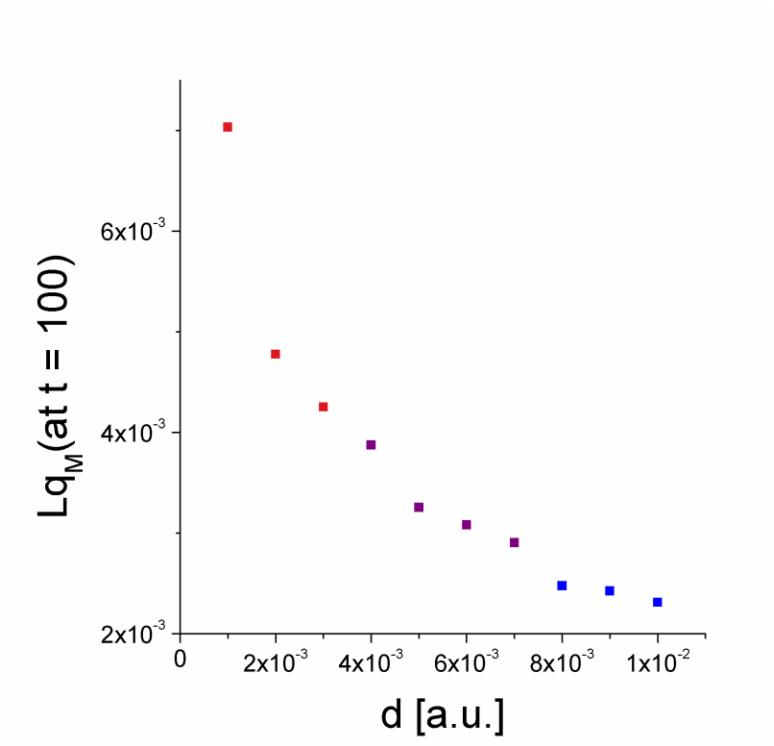


**Supplementary Figure 5. Cellular mobility speeds decomposition in the PDE model.** For the PDE model, the value of $q_M$ after 100 time steps, multiplied by cell size, *L*, is plotted vs. the rate of cellular mobility (random movement akin to diffusion), *d*. As *d* increases, the value of $q_M$ decreases, indicating that the demixing process is further along.

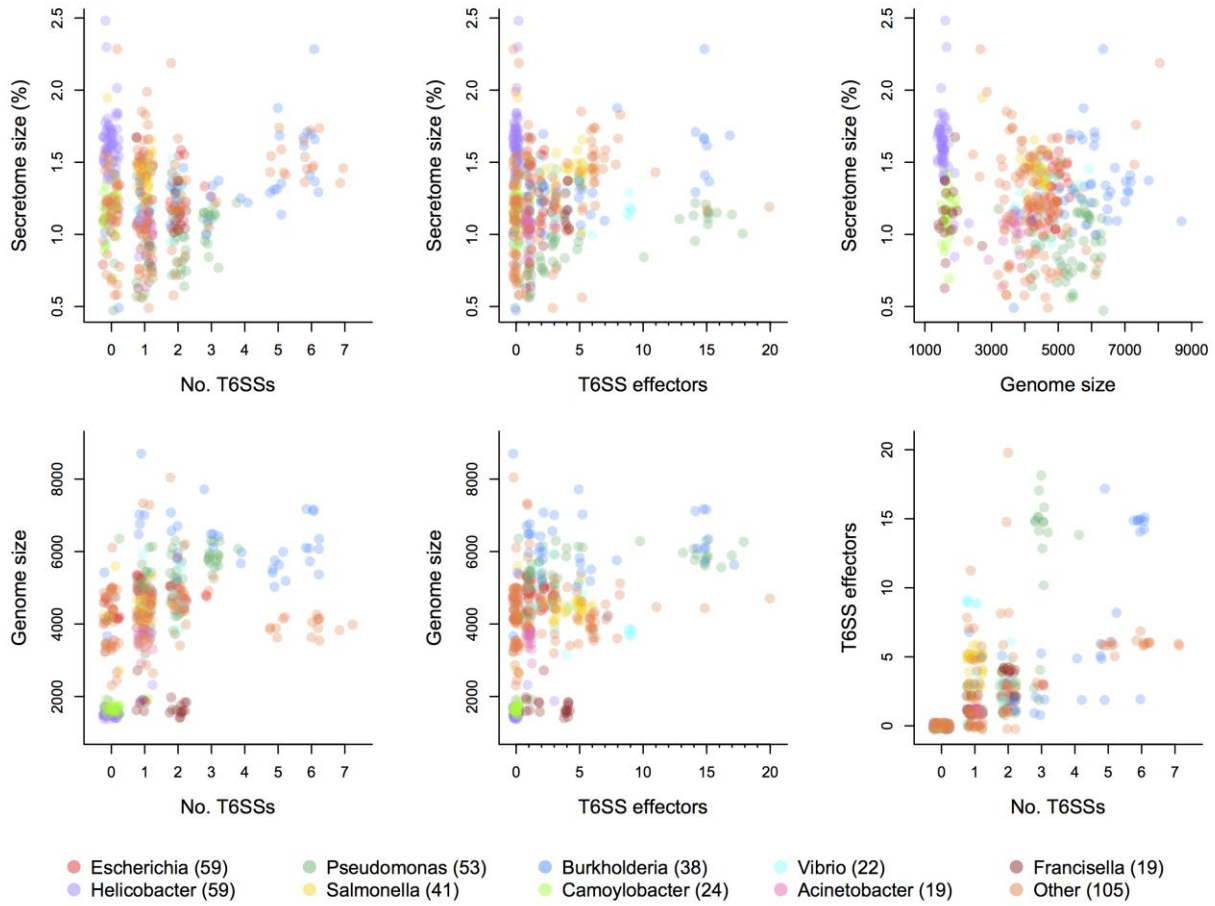


**Supplementary Figure 6. Scatterplots of raw data from comparative analysis.** Shown are pairwise scatterplots of all data included in our comparative analysis. Colours indicate different genera as indicated in the legend.

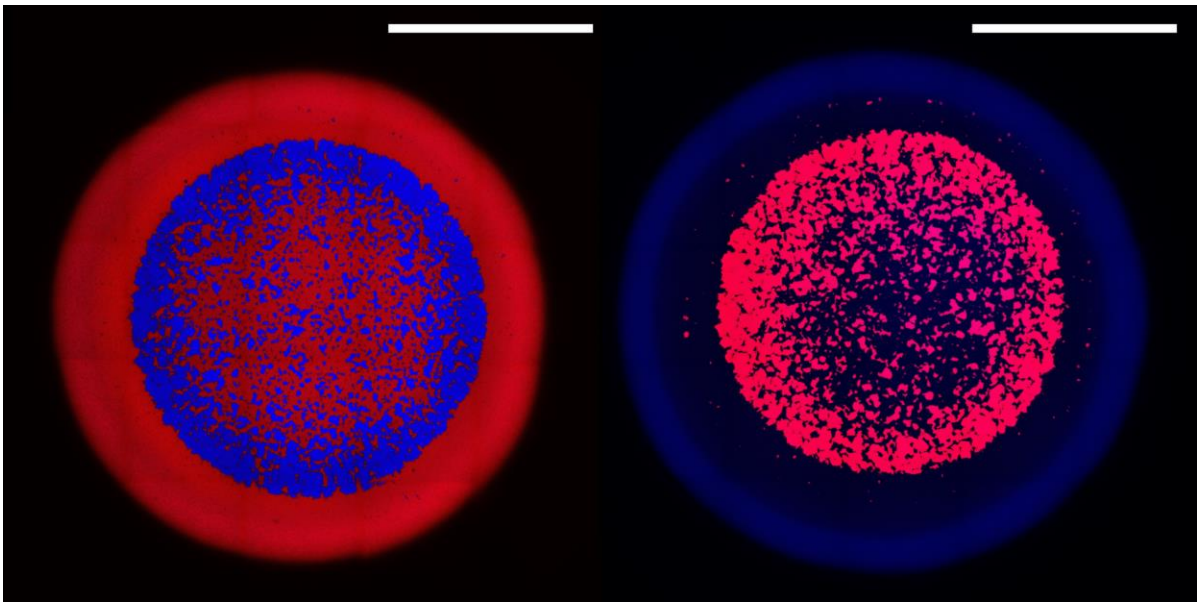

**Supplementary Figure 7. Decomposition is not affected by swapping fluorescence markers.** On the left we show a phase separated colony of *V. cholerae* strain C6706 in red and 692-79 in blue (as we do throughout the paper, GFP is represented in blue to avoid issues with red-green colourblindness). On the right, we show the same two strains, but with the fluorescent markers reversed. These colonies were grown for 24 h at 25°C. The scale bar denotes 1 mm.

**Supplementary Tables**

**Supplementary Table 1:** List of strains used in this study.

| *Vibrio cholerae* strains | Genotype |
|---|---|
| C6706 red T6SS$^+$ | Δ*vc1807*::p*tac-mKO* p*tac-qstR* |
| C6706 red T6SS$^-$ | Δ*vc1807*::p*tac-mKO* p*tac-qstR* Δ*vasK* |
| C6706 green T6SS$^+$ | Δ*vc1807*::p*tac-mTFP1* p*tac-qstR* |
| C6706 green T6SS$^-$ | Δ*vc1807*::p*tac-mTFP1* p*tac-qstR* Δ*vasK* |
| 692-79 red T6SS$^+$ | *lacZ*::p*tac-mKO* |
| 692-79 red T6SS$^-$ | *lacZ*::p*tac-mKO* Δ*vasK* |
| 692-79 green T6SS$^+$ | *lacZ*::p*tac-mTFP1* |
| 692-79 green T6SS$^-$ | *lacZ*::p*tac-mTFP1* Δ*vasK* |

**Supplementary Table 2:** Effects of numbers of T6SSs and T6SS effectors on secretome size.

| **Fixed Terms** | **Parameter Estimate** | **Lower 95% C.I.** | **Upper 95% C.I.** | **$P_{MCMC}$** |
|---|---|---|---|---|
| Intercept | –4.4661 | –4.7097 | –4.2588 | **<0.0001** |
| No. T6SSs | 0.0322 | 0.0085 | 0.0559 | **0.0076** |
| T6SS effectors | 0.0105 | 0.0014 | 0.0194 | **0.0228** |
| **Random Terms** | **Variance** | **Lower 95% C.I.** | **Upper 95% C.I.** | |
| Phylogenetic variance | 0.0833 | 0.0611 | 0.1096 | NA |
| Residual variance | 0.0006 | 0.0002 | 0.0014 | NA |

**Supplementary Table 3:** Effect of number of T6SSs on secretome size.

| **Fixed Terms** | **Parameter Estimate** | **Lower 95% C.I.** | **Upper 95% C.I.** | **$P_{MCMC}$** |
|---|---|---|---|---|
| Intercept | –4.4652 | –4.717 | –4.2313 | **<0.0001** |
| No. T6SSs | 0.0456 | 0.0252 | 0.0672 | **<0.0001** |
| **Random Terms** | **Variance** | **Lower 95% C.I.** | **Upper 95% C.I.** | |
| Phylogenetic variance | 0.0854 | 0.0606 | 0.1102 | NA |
| Residual variance | 0.0007 | 0.0002 | 0.0014 | NA |

**Supplementary Table 4:** Effect of number of T6SS effectors on secretome size.

| **Fixed Terms** | **Parameter Estimate** | **Lower 95% C.I.** | **Upper 95% C.I.** | **$P_{MCMC}$** |
|---|---|---|---|---|
| Intercept | –4.44223 | –4.66215 | –4.22636 | **<0.0001** |
| T6SS effectors | 0.0164 | 0.0084 | 0.0242 | **<0.0001** |
| **Random Terms** | **Variance** | **Lower 95% C.I.** | **Upper 95% C.I.** | |
| Phylogenetic variance | 0.085 | 0.0612 | 0.1102 | NA |
| Residual variance | 0.0007 | 0.0002 | 0.0015 | NA |

**Supplementary Table 5:** Effects of numbers of T6SSs, T6SS effectors and genome size on secretome size.

| **Fixed Terms** | **Parameter Estimate** | **Lower 95% C.I.** | **Upper 95% C.I.** | **$P_{MCMC}$** |
|---|---|---|---|---|
| Intercept | –4.2362 | –5.4144 | –3.0159 | **<0.0001** |
| No. T6SSs | 0.0326 | 0.008 | 0.0564 | **0.01** |
| T6SS effectors | 0.0106 | 0.0021 | 0.0204 | **0.0256** |
| Log genome size | –0.0279 | –0.1777 | 0.1133 | 0.7248 |
| **Random Terms** | **Variance** | **Lower 95% C.I.** | **Upper 95% C.I.** | |
| Phylogenetic variance | 0.0838 | 0.0582 | 0.1074 | NA |
| Residual variance | 0.0007 | 0.0001 | 0.0014 | NA |

**Supplementary References**


1 Bernardy, E. E., Turnsek, M. A., Wilson, S. K., Tarr, C. L. & Hammer, B. K. Diversity of Clinical and Environmental Isolates of *Vibrio cholerae* in Natural Transformation and Contact-Dependent Bacterial Killing Indicative of Type VI Secretion System Activity. *Applied and Environmental Microbiology* **82**, 2833-2842 (2016).